Gene CG15630 (fipi) is involved in regulation of the interpulse interval in Drosophila courtship song

Article *in* Journal of Neurogenetics · December 2017

DOI: 10.1080/01677063.2017.1405000

6 authors, including:

S. A. Fedotov
Russian Academy of Sciences
7 PUBLICATIONS **4** CITATIONS
SEE PROFILE

Julia Bragina
Russian Academy of Sciences
9 PUBLICATIONS **157** CITATIONS
SEE PROFILE

Elena A. Kamysheva
Russian Academy of Sciences
14 PUBLICATIONS **34** CITATIONS
SEE PROFILE

Nikolai Kamyshev
Russian Academy of Sciences
46 PUBLICATIONS **295** CITATIONS
SEE PROFILE

Journal of Neurogenetics

ISSN: 0167-7063 (Print) 1563-5260 (Online) Journal homepage: http://www.tandfonline.com/loi/ineg20

Gene CG15630 (fipi) is involved in regulation of the interpulse interval in Drosophila courtship song

Sergey A. Fedotov, Julia V. Bragina, Natalia G. Besedina, Larisa V. Danilenkova, Elena A. Kamysheva & Nikolai G. Kamyshev

To cite this article: Sergey A. Fedotov, Julia V. Bragina, Natalia G. Besedina, Larisa V. Danilenkova, Elena A. Kamysheva & Nikolai G. Kamyshev (2017): Gene CG15630 (fipi) is involved in regulation of the interpulse interval in Drosophila courtship song, Journal of Neurogenetics, DOI: 10.1080/01677063.2017.1405000

To link to this article: https://doi.org/10.1080/01677063.2017.1405000

Published online: 30 Nov 2017.

JOURNAL OF NEUROGENETICS, 2017
https://doi.org/10.1080/01677063.2017.1405000

Taylor & Francis
Taylor & Francis Group

ORIGINAL ARTICLE

Gene *CG15630* (*fipi*) is involved in regulation of the interpulse interval in *Drosophila* courtship song

Sergey A. Fedotov, Julia V. Bragina, Natalia G. Besedina, Larisa V. Danilenkova, Elena A. Kamysheva and Nikolai G. Kamyshev

Pavlov Institute of Physiology, Russian Academy of Sciences, St. Petersburg, Russia

ABSTRACT

To study the central pattern generators functioning, previously we identified genes, whose neurospecific knockdowns led to deviations in the courtship song of *Drosophila melanogaster* males. Reduced expression of the gene *CG15630* caused a decrease in the interpulse interval. To investigate the role of *CG15630,* which we have called here *fipi* (*factor of interpulse interval*), in the courtship song production, at first, we have characterized *fipi* transcripts and protein (FIPI) in the mutant flies carrying P insertion and deletions in this gene and in flies with its RNAi knockdown. FIPI is homologous to the mammalian NCAM2 protein, an important factor of neuronal development in the olfactory system. In this study, we have revealed that local *fipi* knockdown in the antennal olfactory sensory neurons (OR67d and IR84a), which are responsible for reception of chemosignals modulating courtship behavior, alters the interpulse interval in the opposite directions. Thus, a proper *fipi* expression seems to be necessary for perception of sexual chemosignals, and the effect of *fipi* knockdown on IPI value depends on the type of chemoreceptor neurons affected.

ARTICLE HISTORY
Received 7 February 2017
Revised 4 November 2017
Accepted 10 November 2017

KEYWORDS
Drosophila mutant; PdL excision; Gal4/UAS system; RNA interference; chemosignals; olfactory circuits

Introduction

Elucidation of the morphological and functional organization of neural networks that form the motor program of simple rhythmic actions in animals (motor pattern) is a fundamental scientific problem. Its urgency is determined by the need for modeling and treatment of diseases accompanied with impairment of vital motor functions such as breathing, heartbeat, locomotion, and others. In mammals, the study of the neural mechanisms of motor pattern generation is extremely difficult because of the complexity of neural networks and the heterogeneity of its elements. As a result, the neural networks forming motor patterns have been described mainly at the modular level rather than at the level of individual neurons. One approach to overcome difficulties in the study of generators in mammals consists in molecular labeling of neurons (Andersson *et al.*, 2012; Borgius *et al.*, 2014; Goulding, 2009), whose malfunction is accompanied by abnormalities in the pattern of rhythmic activity. However, the search for molecular markers and investigation of their involvement in the rhythmic activity in mammals may take more than a decade. The research projects conducted on invertebrates are much more effective. For example, the study of *Drosophila na* mutants showing locomotor disorders (Nash, Scott, Lear, & Allada, 2002), together with other studies, led in several years to discovery of the universal molecular component of pacemaker cells, the Na^+ leak channel (Lu & Feng, 2012). A convenient model to explore the molecular mechanisms of motor pattern generation is a neural network that controls wing vibration by a courting *Drosophila* male, producing the pulse courtship song. Simplicity of this behavioral act in conjunction with a variety of molecular and genetic techniques developed for *Drosophila* allowed to establish the neural network for courtship song production and to determine the role of each element in the network (von Philipsborn *et al.*, 2011). Previously, we have reported that the gene *CG15630* determines the frequency of wing beats producing the pulse courtship song (Fedotov *et al.*, 2014). Reduced expression of *CG15630* in neurons was accompanied by a shortening of interpulse interval (IPI). Since it is the most distinctive phenotype for this gene, we have named it *fipi* (*factor of interpulse interval*). Neuronal specificity of the gene expression (Chintapalli, Wang, & Dow, 2007) and its homology to the genes encoding proteins from the families of neural cell adhesion molecules NCAM1 (Ensembl Family ID PTHR10489_SF34) and NCAM2 (PTHR10489_SF35) let us suggest a possible role of *fipi* in such processes as adhesion and proliferation of nerve cells, their migration, neuritogenesis, synaptic plasticity, and regeneration (Burgess *et al.*, 2008; Rutishauser, 2008; Seidenfaden, Krauter, & Hildebrandt, 2006; Walmod, Kolkova, Berezin, & Bock, 2004). Thus, *fipi* is presumably an important molecular factor of a neural network that determines the motor pattern of *Drosophila* male courtship song.

In this study, we aimed to investigate the mechanisms of *fipi* involvement in establishing the IPI in male courtship song. We have characterized the transcripts and the protein

CONTACT Sergey A. Fedotov serg900@yandex.ru Makarova emb., 6, 199034 Saint-Petersburg, Russia

encoded by *fipi*, as well as deviations of *fipi* expression in the mutants and knockdowns. Behavioral analysis of (1) the mutant with insertion of P element at the beginning of *fipi*, (2) the mutant with deletion of significant part of the *fipi* first exon, and (3) the RNAi mediated knockdown of this gene revealed functional significance of the *fipi* first exon integrity and *fipi* transcript/protein level for keeping the IPI value in the normal range.

In experiments with the local *fipi* knockdowns in various types of neurons we have determined that olfactory sensory neurons (OSN) are the probable neuronal substrate mediating *fipi* involvement in IPI setting. *fipi* knockdown in distinct populations of OSNs detecting aphrodisiac (IR84a receptor) and antiaphrodisiac (OR67d receptor) resulted in opposite IPI deviations. Our data indicate the necessity of a proper *fipi* expression level for regulatory influences from the OSNs detecting sex pheromones on the courtship song pattern.

Materials and methods

Experimental subjects

Five-days-old *Drosophila melanogaster* males were used in all experiments. The rearing and experimental conditions were described previously (Fedotov *et al.*, 2014). Wild-type strain Canton-S (CS) derived from the Bloomington Drosophila Stock Center (BDSC, Bloomington, IN). The line *w*;P{PdL}CG15630[3404z]*, carrying the insertion of *PdL* transposon with *mini-white* gene inside (Bieschke, Wheeler, & Tower, 1998; Landis, Bhole, Lu, & Tower, 2001) into *CG15630 (fipi)* gene, was created earlier (Fedotov *et al.*, 2014) by remobilization of the transposon from the X chromosome. The initial *PdL(X)* line was a gift from Prof. John Tower (University of Southern California, USA). To use CS strain as a control, this line was back crossed for 10 generations to the 'cantonized' w[1118] line yielding the *w[1118];P{PdL}CG15630[3404z]* flies used in the experiments (mentioned hereafter as fipi[3404z]). The lines fipi[361] and fipi[362] with precise and imprecise excision of *PdL* transposon, respectively, were created by its remobilization from the *fipi* gene. In fipi[361], sequencing of a region around the site of *PdL* insertion showed removal of the transposon with restoration of *fipi* canonical sequence. In fipi[362], the part of the first *fipi* exon downstream from the site of *PdL* insertion together with a part of the first intron were deleted (Figure 1). The coordinates of the 719 bp deletion determined by sequencing were 2L: 4793237..4793955, according to the FlyBase version FB2016_01, released 14 January 2016. To enhance the production of courtship song by males of both excision lines, fipi[361] and fipi[362], the additional crosses were made to substitute the *w[*]* for *w[+]* allele in the X chromosome. In all experiments, the line fipi[361] with precise *PdL* excision served as a control to the mutant fipi[362]. Males with *fipi* knockdown derived from the crossing of females, carrying the *GAL4* transgene expressed under control of a specific gene promoter (driver), with males, carrying the *UAS* transgene producing interfering RNA to *fipi*

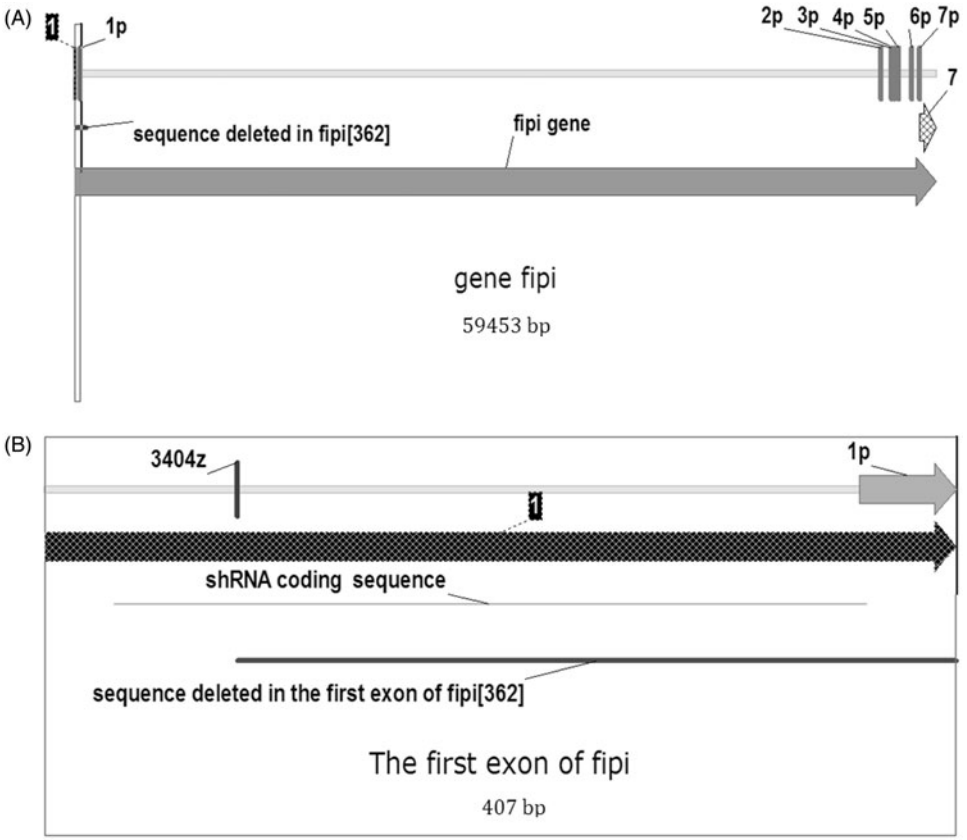

Figure 1. Scheme of the gene *fipi* (A) and its first exon (B). The numbers 1 and 7 designate the first (outlined by frame) and last exons, 1p–7p stand for the coding parts of exons. The pointer 3404z shows localization of the insertion P{PdL}CG15630[3404z].

(RNAi stock). Stocks with GAL4 drivers were obtained from BDSC: nompC-GAL4 (#36361, *y[1]w[*];PBac{y[+mDint2] w[+mC]=nompC-GAL4.P}VK00014;Df(3L)Ly,sens[Ly-1]/ TM6C,Sb[1]*); ppk-GAL4 (#32078, *w[*]; P{w[+mC]=ppk-GAL4.G}2*); Snmp-GAL4 (#51305, *w[118]; P{w[+mC]=Snmp-VP22-GAL4.5. 412}2*); Ddc-GAL4 (#7009, *w[1118];P{w[+mC]=Ddc-GAL4.L}4.36*); D42-GAL4 (#8816, *w[*];P{w[+mW.hs]= GawB}D42*); ChAT-GAL4 (#6798, *w[1118]; P{w[+mC]= ChAT-GAL4.7.4}19B/CyO, P{ry[+t7.2]=sevRas1.V12}FK1*), Or47b-GAL4 (#9983, *w[*]; P{w[+mC]=Or47b-GAL4.7.467}15.5A*), Or67d-GAL4 (#9998, *w[*]; P{w[+mC]=Or67d-GAL4.F}57.2*), Ir84a-GAL4 (#41750, *w[*]; TI{GAL4}Ir84a[GAL4]*).

Act5C-GAL4 driver (*w[1118]; P{w[+mC]=Act5C-GAL4} 25FO1/CyO, y[+])* was kindly provided by Prof. Konstantin G. Iliadi (Hospital for Sick Children, Toronto, Canada). The RNAi stock, *y,w[1118]; P{KK107002}VIE-260B* (#107797), denoted hereafter as UAS-RNAi, with transgene coding for interfering long hairpin RNA (hpRNA) to the gene *fipi* placed under *UAS* control, and the host stock for KK RNAi lines *y,w[1118]; P{attP, y[+],w[3′]* (#60100) were obtained from Vienna Drosophila RNAi Center (VDRC, Austria). The offspring from crosses between the corresponding GAL4 driver and the host stock #60100 served as a control for knockdowns. Earlier, we have shown that there is no difference in IPI between offspring from CS × #60100 and CS × #107797 crosses that indicates the absence of own effect of the UAS-RNAi insertion on IPI (Fedotov *et al.*, 2014). For detection of olfactory neuronal structures in confocal microscopy the stock with *UAS-GFP* transgene was used (#32202, w[*]; P{w[+mC] = 10XUASIVS-GFP-WPRE}attP2, BDSC).

Courtship songs assay and analysis

Recording and analysis of courtship song were described previously (Fedotov *et al.*, 2014; Iliadi *et al.*, 2009; Popov, Savvateeva-Popova, & Kamyshev, 2000). In short, a male was placed, together with a fertilized female, into an experimental thermostated chamber placed above the microphone, and the sounds were recorded for 5 min at 25 °C. The sensitive band microphones and low-noise microphone amplifiers were constructed in compliance with Bennet-Clark's recommendations (Bennet-Clark, 1984) with small scheme modifications in the workshop of the Department of Genetics of Wurzburg University by the engineer K. Ochsner with financial support of Prof. P. Riederer. The sound records were analyzed using the program 'Drosophila courtship song analysis' (DCSA, © N.G. Kamyshev), which automatically recognized the pulse song and calculated its various parameters. Automatic pulse recognition in sound records (wav files, mono, 44,100 Hz, 16 bit) was based on parameters, empirically selected when analyzing natural pulse song, and applied at successive stages of analysis. In 16-bit sound records the amplitude may vary from −32767 to +32767 arbitrary units (a.u.). Firstly, all fragments of a sound record containing the absolute values of the amplitude exceeding the noise threshold (1200 a.u.) and flanked with noise of sufficient duration were found. The minimal noise duration of 30 data points (~0.68 ms for 44,100 Hz records) was used to distinguish the true noise from subthreshold fluctuations within potential pulse. For each fragment found, the following parameters were used to distinguish the song pulse from other signals above the noise threshold. The minimal positive or negative peak amplitude of 1600 a.u. was established. The sharpness of both positive and negative peaks was estimated by calculating the ratio of the maximum absolute amplitude to the number of data points between the peak and preceding zero line crossing (the tangent of the slope angle). The tangent value >30.0 was used to recognize the song pulses. The fragments, where there were more than seven zero line crossings, were considered as signals having no relation to song pulses. If two pulses were separated by 20 ms or less, the pulse with lower amplitude was ignored. Pulse positions in adjacent pulses were defined using peaks of the same type, either positive or negative, depending on what peak was more pronounced in the first pulse. The pulses are usually organized in trains consisting of two or more pulses. The pulses separated by 80 ms or less were ascribed to one train, and IPI values were calculated only for intra-train pulses. Despite the algorithm described above recognized almost all song pulses, a manual correction was required, mainly to delete some unrelated signals. That was made in the editor mode by successive viewing of all highlighted signals recognized by the program as pulse song. The mean duration of the pulse train (ms), the frequency of trains initiation (trains per 100 s), and the mean IPI within a train (ms) were calculated for each experimental male and used in further statistical analysis. The statistical comparisons were performed by randomization test (Edgington, 1995) at the confidence level $\alpha = 0.95$. The 95% confidence intervals were calculated by the bias-corrected and accelerated (BCa) bootstrap using the IBM SPSS Statistics 20 (Armonk, NY) software (10,000 iterations, Efron & Tibshirani, 1993).

Real-time RT-PCR

Assay of *fipi* expression level was performed as described previously (Fedotov *et al.*, 2014). Briefly, the total RNA was isolated from males and transcribed to cDNA using the reverse transcriptase. cDNA samples served as a template in the quantitative real-time PCR with a fluorescent dye EvaGreen® (Biotium, BT-31000). Two pairs of primers were used to assess the level of transcripts comprising the first and second *fipi* exons (RT1, 5′-ATTCGTTGAGATTCT CGCAATGCG-3′, 5′-CGGCGATTTCCAATGGAGCT-3′), and transcripts containing the fifth and sixth *fipi* exons (RT2, 5′-GGCCGATGGTTTGCTCATCAAC-3′, 5′-AGTAGC TGTCCGACTGGATCGTGTA-3′, Figure 2). The expression level of *RpL32* was used as an internal control. Statistical analysis was performed with randomization test in the program REST 2009 at the confidence level $\alpha = 0.95$ (Pfaffl, Horgan, & Dempfle, 2002).

Northern blot

Three micrograms of total RNA from males were separated by electrophoresis in 1% denaturing agarose gel

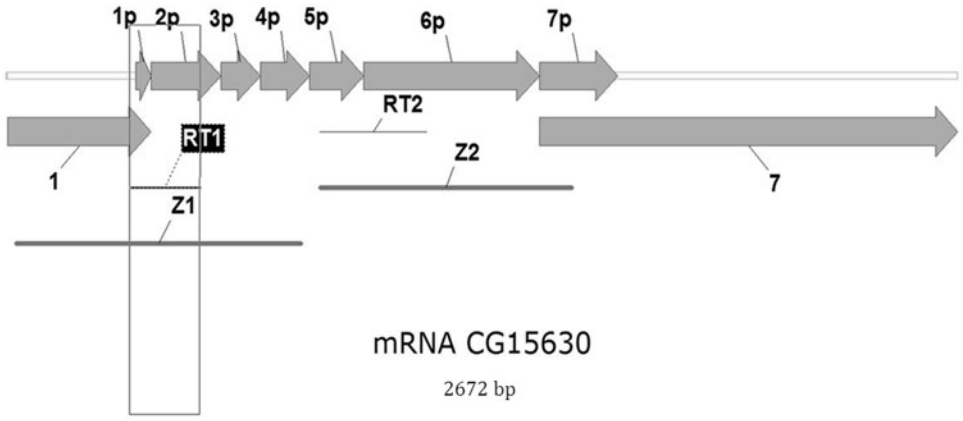

Figure 2. The annotated *fipi* mRNA (FlyBase, FB2016_01, released 14 January 2016). The numbers 1 and 7 designate the first and the last exons, 1p–7p are the coding parts of *fipi* exons. RT1 and RT2 are the fragments amplified in the real-time RT-PCR, Z1 and Z2 indicate the regions complementary to RNA probes 1 and 2 used in the northern blot.

(4-morpholinepropanesulfonic acid (MOPS) buffer, 2.2 M formaldehyde). Before loading to the gel, samples and ladder (#SM1823, Thermo Fisher Scientific, Waltham, MA) were denatured in RNA loading mix (MOPS buffer, 2.2 M formaldehyde, 70% formamide, 0.001% EtBr) and mixed with 1/5 volume of 5× RNA gel buffer (50% glycerol, 1 mM EDTA, 0.1% bromophenol blue, 0.1% xylene cyanole). After electrophoresis, the gel was washed from formaldehyde, and position of marked RNA bands was determined using the gel documentation system. Capillary RNA transfer from the gel to a nylon membrane (N-8522, Sigma-Aldrich, St. Louis, MO) was carried overnight in 20× SSC buffer (3 M sodium chloride, 0.3 M sodium citrate, pH 7.0). RNA was crosslinked to the membrane by UV irradiation (BIO-LINK® BLX, 0.06 J/cm^2), and then pre-hybridization was carried out for two hours at a temperature of 53 °C in HSB buffer (7% SDS, 50% formamide, SSC 5×, 2% skimmed milk, 50 mM sodium phosphate, pH 7.0, 0.1% *N*-lauroylsarcosine Na, 50 µg/ml salmon sperm DNA). Under the same conditions, hybridization was performed overnight in HSB with denatured RNA probes Z1 and Z2 or the complementary to Z2 control probe K2 at a concentration of 5 ng/ml (Figure 2). After hybridization, washing of the membrane was performed as follows: 2 × 15′, 25 °C, 2× SSC, 0.1%, SDS and 2 × 15′, 68 °C, 0.5× SSC, 0.1% SDS. The membrane was blocked 60 min in 1% skimmed milk in the maleic buffer and incubated in anti-digoxigenin antibody conjugated with alkaline phosphatase (#11093274910 ROCHE, Sigma-Aldrich, 1:15,000 in 1% skimmed milk, maleic buffer). Antibody was discarded, and membrane was washed twice for 15 min in maleic buffer with 0.2% Tween-20 and then equilibrated with a detection buffer (0.02 M Tris HCl, pH 9.8, 1 mM magnesium chloride). Chemiluminescent detection was performed using the CDP-Star reagent (T2145, TFS). Then, to correct the load of RNA in each sample, the membrane was rinsed in water, and hybridization with the RNA probe R1 to the ribosomal 28Sa RNA was carried out.

RNA probes were synthesized by *in vitro* transcription using a mixture of NTPs with addition of digoxigenin-11-uridine-5′-triphosphate (DIG-RNA labeling mix, #11277073910 ROCHE, Sigma-Aldrich). Templates for the transcription were DNA fragments amplified by PCR using cDNA and primers with T7-polymerase promoter at the 5′ end. The following primers were used (the T7-promoter is written in italics): Z1for – 5′-CGGTTCACCTACACTTCGTG-3′, Z1rev – 5′-*TAATACGACTCACTATAGGG*TGAAGTGCCAGGTGACATTC-3′, Z2for – 5′-CGATGGTTTGCTCATCAACA-3′, Z2rev – 5′-*TAATACGACTCACTATAGGG*GTGAAGTCACTGAATCCGGC-3′, K2for – 5′-*TAATACGACTCACTATAGGG*CGATGGTTTGCTCATCAACA-3′, K2rev – 5′-GTGAAGTCACTGAATCCGGC-3′, R1for – 5′-CTTAGAGGTTAAGCCCGATGA-3′, R1rev – 5′-*TAATACGACTCACTATAGGG*CCTCTAATCATTCGCTTTACCA-3′.

Qualitative estimation of transcripts level in the northern blot was performed by comparing bands intensity using the ImageJ software.

Procedures in identification of 5000 bp fipi *transcript*

The total RNA was isolated from males, transcribed to $cDNA_{N9}$ using the RevertAid H Minus Reverse Transcriptase (#EP0452,Thermo Fisher Scientific) and random nonamer primers. $cDNA_{N9}$ samples served as a template in the PCR amplification of *fipi[361]* and *fipi[362]* transcript fragments with 'D' polymerase (mix of Taq and Pfu polymerases, Beagle, Saint Petersburg, Russia) and Long PCR Enzyme Mix (#K0182,Thermo Fisher Scientific). Four primers were used to assess the integrity and sizes of the *fipi* regions: from exon 1 (primer Z1for), exon 2 (primer gsp2for, 5′-GAATCCCTCATCGTCCAGTG-3′) and exon 5 (primer Z2for) to exon 7 (primer Z2rev), see Figure 6(D).

5′-RACE was performed according to protocol of Huang and Chen (2006) with a few modifications. Briefly, first-strand $cDNA_{GSP}$ was synthesized using the *fipi* specific primer GSP2-RT (5′-GTCCTTTGTGCTCGCGTA-3′) and T–S primer containing G residues at the 3′ most part (5′-CACCATCGATGTCGACACGCGTCGGG-3′). The $cDNA_{GSP}$ was amplified in PCR using the T–S primer and GSP2-RT with 'D' polymerase. PCR products were phosphorylated, self-ligated and used as templates for inverse PCR performed with outward primers specific to the exon 2 (gsp2for, gsp2rev 5′-TACCGCACCACGCTGTG-3′). The inverse PCR products were used in the second round (nested) PCR

with primers gsp2forNest 5′-GCAGTCCCGATCCCAAA-3′ and gsp2revNest 5′-GGACTGAGGGAAAGGCTCT-3′, see Figure 6(E).

PCR products along with a 1 kB DNA ladder (#M11, SibEnzyme, Novosibirsk, Russia) were visualized by ethidium bromide staining on a 0.8% TAE agarose gel.

Western blot

Electrophoretic separation of proteins was performed in 10% polyacrylamide gel under denaturing conditions. Males were frozen for one hour at −20 °C, then the whole flies or their distinct body parts were homogenized with a pestle in the lysis buffer (50 mM Tris-Cl, pH 8.0, 1% Triton X-100, 150 mM NaCl, complete protease inhibitor cocktail, Roche). To equalize approximately the protein concentration in various types of samples, it was measured using the Bradford's method. According to this estimation, the samples were prepared from either 6 *Drosophila* males, or 60 heads, or 16 thoraxes, or 12 abdomens in 200 µl of the lysis buffer. Homogenized samples were heated at 95 °C for 5 min, centrifuged 5 min at 13,000 rpm, and 10 µl of supernatant was loaded onto the gel (∼5 µg of total protein). PageRuler prestained protein ladder (#26616, Thermo Fisher Scientific) and Prestained protein molecular weight marker (#26612, Thermo Fisher Scientific) was used to determine the molecular weight of the polypeptide encoded by the gene *fipi*. Protein transfer from the gel to a nitrocellulose membrane was performed in the Mini Trans-Blot chamber (Bio-Rad, Hercules, CA). The transfer efficiency and equal loading were confirmed by Ponceau S staining. Membrane was blocked at 4 °C overnight in 5% solution of skimmed milk in TBST (20 mM Tris-Cl, pH 7.5, 150 mM NaCl, 0.1% Tween-20). The next day membrane was rinsed and washed with TBST, 4 × 10′. All washes were carried uniformly, at room temperature (RT) with shaking (250 rpm). Primary antibodies 32II against FIPI (polypeptide encoded by *fipi*) were created by immunization of rabbits with oligopeptide RSPDPKVELHWKSP (the second *fipi* exon, 47–60 aa, FlyBase). The primary antibodies were diluted (1:2000) in 5% solution of skimmed milk in TBST and incubated with membrane for 2 h at 22 °C with shaking. Membrane incubation with secondary antibodies conjugated with horseradish peroxidase (HRP, #A16104, Thermo Fisher Scientific) was performed in the same manner. After hybridization, the membrane was washed in TBST and ECL™ Prime Western Blotting Detection Reagent (#RPN2232, GE Healthcare, Chicago, IL) was used for chemiluminescent detection of peroxidase activity on a film (Carestream Health MXBE, Kodak, Rochester, NY).

For quantitative analysis of FIPI level band intensity values were corrected with cysteine string protein (CSP, load control), normalized as proportion of control meanings and averaged of four independent experiments.

Confocal microscopy

Males were immobilized by cold anesthesia, and brain and antennas were dissected in the cold phosphate buffer (Fore *et al.*, 2011; Karim, Endo, Moore, & Taniguchi, 2014). Samples were fixed with 4% formaldehyde in 0.1% PBST (PBS with 0.1% Triton X-100) for 20 min at RT with shaking (250 rpm) followed by washes in 0.4% PBST (PBS with 0.4% Triton X-100), 4 × 20′ at RT with shaking (washes were uniform unless otherwise stated). Samples were blocked with 5% goat serum in 0.1% PBST for 40 min at RT on a shaker and hybridized with primary antibodies in 5% goat serum, 0.1% PBST, three days at 4 °C with shaking. Primary antibodies against FIPI (32II, 1:500, rabbit), CSP (DCSP-1, DSHB, 1:20, mouse), and GFP (338001, BioLegend, 1:250, rat) were used. CSP antibody stained neuropile structures in the brain. After washing off the primary antibodies, the samples were incubated in the dark at 4 °C on a shaker for two days with the secondary antibody with fluorescent label dissolved in 5% goat serum, 0.1% PBST. Secondary antibodies were Cy3 anti-rabbit IgG (406402, BioLegend, 1:1000, donkey), Alexa Fluor 647 anti-mouse IgG (ab150115, Abcam, 1:500, goat), Alexa Fluor 488 anti-rat IgG (112–545-003, Jackson, 1:500, goat). The samples were successively washed in 0.4% PBST and PBS (3 × 1′, 2 × 5′) and enclosed into a chamber, made from cover glasses on the slide, filled with GDP (70% glycerol, 2.5% DABCO in PBS). For staining the nuclei, DAPI (4′,6-diamidino-2-phenylindole) was added at concentration 300 ng/ml in the second 0.4% PBST wash.

Fluorescence analysis was carried out on the confocal laser scanning microscope LSM 710 (Carl Zeiss, Oberkochen, Germany) in the confocal microscopy center of Pavlov Institute of Physiology. Images were fixed at 10×, 20×, 63×, and 100, magnification, with scanning steps of 1–5 µm, approximate resolution of 0.5–1 pixel/µm, and averaging the fluorescence over two repeated measurements for a pixel. Laser and filter settings matched the preset values for Cy3, Alexa Fluor 488, Alexa Fluor 647, DAPI in software ZEN 2009 (Carl Zeiss). Analysis and editing of the images was carried out in the free version of ZEN 2011 (black edition, 64 bit, Carl Zeiss).

Results

Courtship song deviations in males with impaired fipi expression

Song activity was estimated in *Drosophila* males with (1) insertion of P element in the first *fipi* exon, (2) partial deletion of the first exon and first intron in the gene, and (3) the *fipi* knockdown in the whole organism through synthesis of hpRNA, interfering the *fipi* expression in the GAL4/UAS system under control of the actin driver, Act5C-GAL4 (Figure 3). In all three cases, there was a decrease in IPI in the pulse song of *Drosophila* males.

fipi expression level

Deviations in *fipi* expression in the experimental flies were assessed by real-time RT-PCR. The expression level of *fipi*, estimated by amplification of RT1 (the first and second

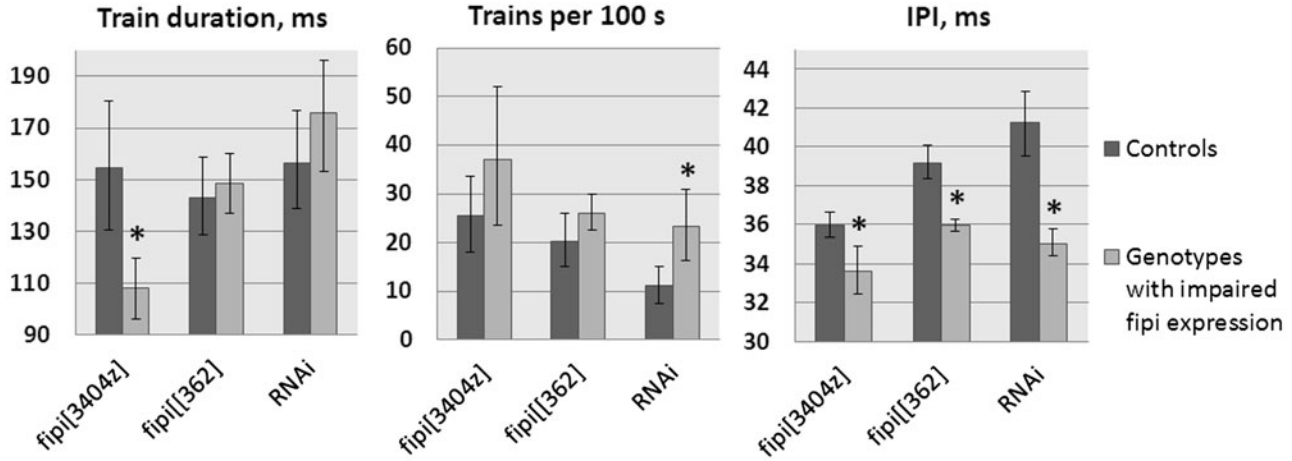

Figure 3. Pulse song parameters in *Drosophila* males with impaired fipi expression. Horizontal axis: fipi[3404z] is the mutant with P insertion in the first *fipi* exon (*w[1118];P{PdL}CG15630[3404z]*); fipi[362] is the imprecise excision of P element with partial removal of the first exon and first intron in *fipi*; RNAi stands for *fipi* knockdown by interfering RNA synthesis in the GAL4/UAS system under control of the Act5C-GAL4 driver (*Act5C-Gal4; P{KK107002}VIE-260B*). For description of the control genotypes see 'Materials and methods' section. Mean values ($n = 40$) with 95% confidence intervals are shown. Significant differences from the corresponding control are marked with asterisks (two-sided randomization test, $p < .05$).

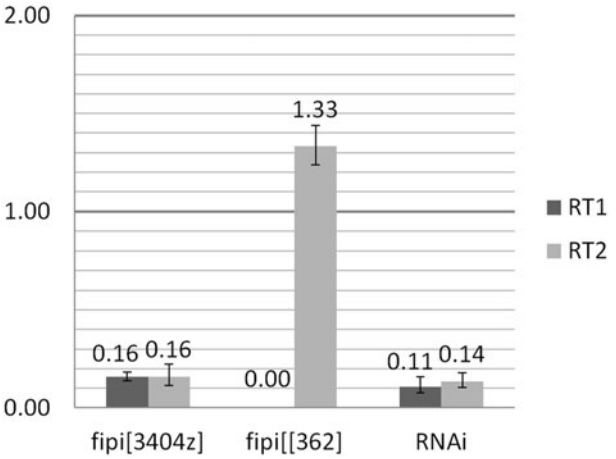

Figure 4. Relative level of *fipi* mRNA determined by real time RT-PCR. RT1 and RT2 define primers used for amplification of different cDNA regions: RT1 for the first and second exons, RT2 for the fifth and sixth exons (see Figure 2). The changes from control values, taken as a unit (1.00) in each case, are shown ($n = 6$). All changes are statistically significant (two-sided randomization test, $p < .05$). For other explanations, see caption for Figure 3.

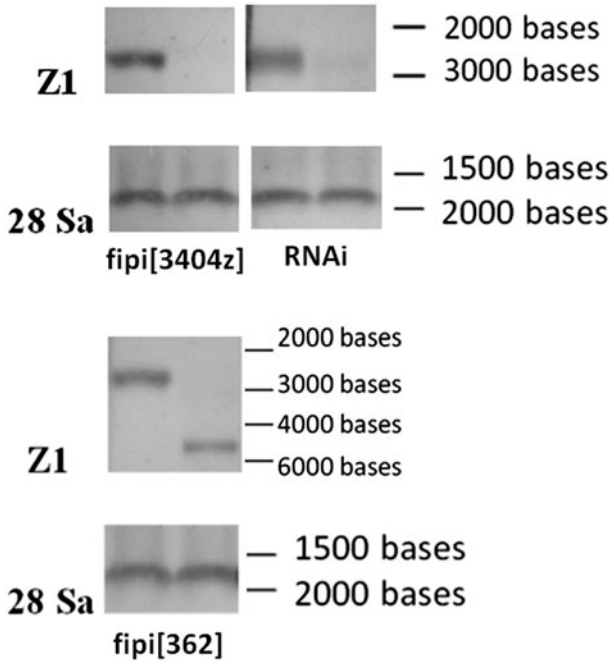

Figure 5. *fipi* transcripts detected with Z1 RNA probe (exons 1–4). Ribosomal 28Sa RNA was used as a load control. Approximate *fipi* transcript sizes are 2700 bp in the control flies (left lanes) and 5000 bp in flies with *fipi[362]* deletion (right lane). For other explanations, see caption for Figure 3.

exons) and RT2 (the fifth and sixth exons) gene regions, was drastically reduced in the knockdown and P insertion flies (Figure 4). *fipi[362]* deletion includes the landing sequence for primer used in RT1amplification (Figures 1 and 2), thus the signal is absent in this case. However, RT2 amplification shows that *fipi* expression level is, conversely, slightly increased in fipi[362] flies.

The transcript produced in fipi[362] should be abnormal due to partial deletion of the first exon and first intron. We have suggested that *fipi* pre-mRNA is synthesized in fipi[362], but the lack of the deleted sequence prevents normal splicing. It is likely that the process of cutting out the first intron, whose size is 55184 bp, is affected (Figure 1). However, the abnormal transcript seems to retain the fifth and sixth exons, and splicing between them operates properly, as we have not detected changes in the melting parameters in real time RT-PCR by EvaGreen fluorescence.

fipi *transcripts*

To assess possible effects of the deletion in fipi[362] flies on *fipi* pre-mRNA splicing, northern blot analysis with two RNA probes, Z1 and Z2, was carried out. Z1 probe has a nucleotide sequence complementary to exons 1–4 in *fipi* mRNA. Z2 is complementary to exons 5–7. In the control line (fipi[361]), both probes detected a transcript with size of approximately 2700 bp (Figure 5, data shown for Z1). Transcript 2700 corresponds to the predicted annotated *fipi* mRNA (2672 bp, *CG15630-RA*, Flybase). In the flies with deletion (fipi[362]), the probes detected a transcript of approximately 5000 bp, while 2700 bp transcript was absent. At the same time, the *fipi* knockdown with hpRNA

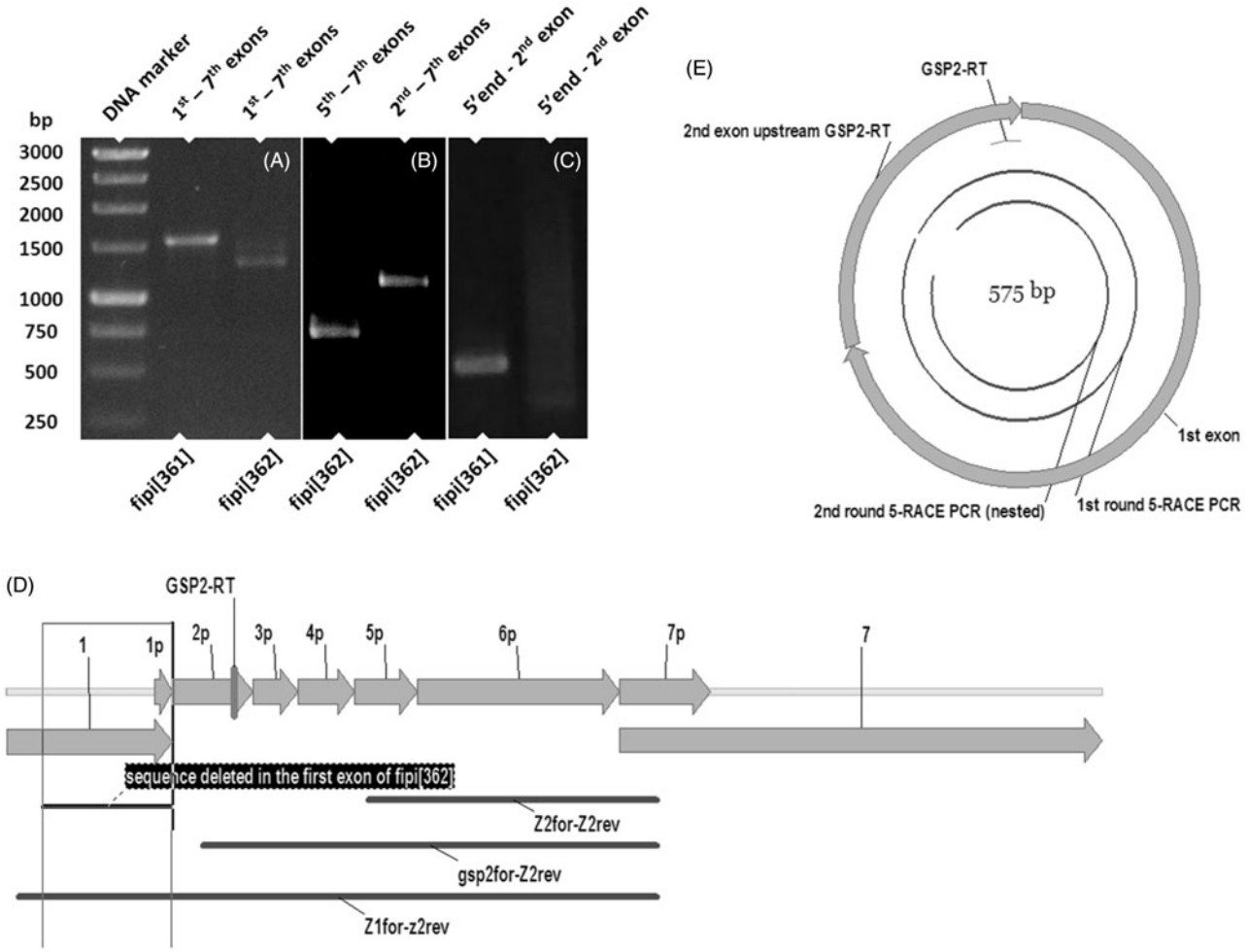

Figure 6. PCR fragments of different regions in the *fipi[361]* and *fipi[362]* transcripts. (A) Results of $cDNA_{N9}$ (synthesized in reverse transcription with random primers) PCR with primers Z1for (beginning of exon 1) and Z2rev (coding part of exon 7). (B) Results of $cDNA_{N9}$ PCR with primer pairs gsp2for (middle of the exon 2)/Z2rev and Z2for (beginning of the exon 5)/Z2rev. (C) Results of the 2nd round of 5′-RACE PCR with inverted primers gsp2forNest/gsp2revNest (second exon) and self-ligated $cDNA_{GSP}$ (synthesized in reverse transcription with reverse primer GSP2-RT). Position of GSP2-RT primer is indicated in (D) and (E). (D) Correspondence between *fipi* mRNA and PCR fragments for the primer pairs specified in (A) and (B). (E) Correspondence between *fipi* mRNA and PCR fragments for primer pairs gsp2for/gsp2rev (1st round 5′-RACE PCR) and gsp2forNest/gsp2revNest (2nd round 5′-RACE PCR).

complementary to the first exon, as well as the P insertion in the first exon, considerably reduced 2700 bp transcript level (Figure 5, Z1 and Z2 showed identical results); other transcripts were not detected in these cases. We suppose that the deletion impairs the recursive splicing, the process when large introns are removed by multiple steps of re-splicing at ratchet points – 5′ splice sites recreated after splicing. A ratchet point was revealed in the *fipi* first intron (Duff *et al.*, 2015), thus the 5000 bp transcript may be an abnormal *fipi* mRNA with incomplete removal of the first intron.

We tried to identify a 5000 bp transcript. By RT-PCR, we first determined that PCR fragments between the second and seventh exons (about 1100 bp, Figure 6(B)) and the fifth and seventh exons (about 700 bp) in *fipi[362]* transcript corresponded to annotated *fipi* mRNA sequence (Figure 6(D)). However, amplification of the fragment between the retained 5′-end portion of the first exon and the seventh exon in fipi[362] flies exhibited only a weakly expressed fragment, about 1400 bp in size (Figure 6(A)). In fipi[361] flies, the clearly expressed fragment between the first and seventh exons was about 1550 bp, that corresponded to bioinformatic data (1557 bp, Figure 6(D)). We had assumed that RT-PCR of 5000 bp transcript failed due to some features of its sequence at 5′-end upstream of the second exon. 5′-RACE was performed to establish the sequence of the 5′-end structure of *fipi[362]* transcripts. The protocol of Huang and Chen (2006) was used with a few modifications. The $cDNA_{GSP2}$ was obtained in a reverse transcription reaction with reverse primer GSP2-RT to the end of the second exon (Figure 6(D)), self-ligated, and two rounds of PCR were performed with inverse primers to the second exon (Figure 6(E)). In fipi[361] flies, the expected fragment of about 550 bp was identified (Figure 6(C)), whose sequencing confirmed its correspondence to the first and second exons of the annotated *fipi* transcript. But only an indistinctly expressed fragment, about 400 bp in size, was detected in fipi[362] flies. We have concluded that a 5000 bp transcript described in the northern blotting experiment possibly contains a region of the first intron that blocks the reverse transcription and do not allow identification of this transcript by standard approaches.

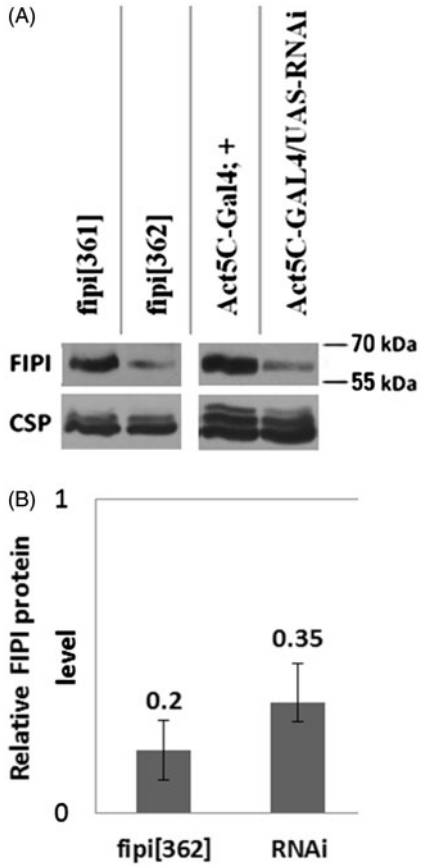

Figure 7. Detection of FIPI protein by western blotting with antibodies against peptide encoded by a sequence in the second *fipi* exon. (A) Samples from heads of the *Drosophila* males with *fipi[362]* deletion, *fipi* knockdown (Act5C-GAL4/UAS-RNAi), and their corresponding controls. The cysteine string protein (CSP) was used as a load control. (B) The changes from control values, taken as a unit (1.00) in each case, are shown. Relative level of FIPI protein was calculated by comparing band intensity using the ImageJ software. The 95% confidence intervals were plotted ($n = 4$, BCa bootstrap, the IBM SPSS Statistics 20 software). For other explanations, see caption for Figure 3.

Characterization of the protein encoded by gene fipi

Polyclonal antibodies against peptide encoded by a sequence in the second *fipi* exon were used for detection of the *fipi* gene product (protein FIPI) in western blotting (see 'Materials and methods' section). In Flybase, the molecular weight of the annotated polypeptide encoded by the gene *fipi* is 50.7 kDa. In control flies fipi[361] and Act5C-GAL4/+, the protein of approximately 62 kDa was recognized (Figure 7(A)) in the head homogenate, but was absent in the samples of thoraces and abdomens. Control application of preimmune serum gave only slight nonspecific staining (data not shown). Analysis of FIPI band intensity in flies with reduced amount of *fipi* mRNA (*fipi* knockdown Act5C-GAL4/UAS-RNAi) and in the deletion stock with *fipi* transcripts of 5000 bp (fipi[362]) revealed its significant decrease relative to the corresponding controls (Figure 7(B)).

IPI deviations in fipi *knockdowns in different populations of nervous cells*

To establish the types of neurons, where abnormal *fipi* expression leads to deviations in IPI, we tested flies with *fipi* knockdown under control of specific GAL4 drivers causing interfering hpRNA synthesis in monoaminergic, cholinergic, motor and sensory (olfactory and mechanosensory) neurons. It was found that the effect of *fipi* knockdown on IPI was not associated with *fipi* suppression in dopaminergic and motor neurons (Figure 8). At the same time, *fipi* knockdown in the population of olfactory neurons (Snmp-GAL4 driver) led to IPI reduction. A similar knockdown effect was revealed with GAL4 drivers, triggering RNA interference in cholinergic neurons (ChAT-GAL4) and in the peripheral sensory neurons (ppk-GAL4).

To specify the involvement of olfactory neurons in mediating the *fipi* knockdown effect on IPI value, we tested the song activity of flies with *fipi* knockdown in three populations of olfactory sensory neurons (OSN) using the drivers Or47b-GAL4, Or67d-GAL4 and Ir84a-GAL4 (Figure 9). Each of these OSN populations demonstrates activity in response to substances that affect *Drosophila* courtship behavior (Dweck *et al.*, 2015; Grosjean *et al.*, 2011; Kurtovic, Widmer, & Dickson, 2007) and projects into the glomeruli of antennal lobes (Stockinger, Kvitsiani, Rotkopf, Tirián, & Dickson, 2005). Snmp-GAL4, which caused IPI reduction when steering *fipi* RNA interference (Figure 8), drives expression in nine glomeruli, including DA1 and VA1l/m, where O67d and Or47b OSNs projects, respectively (Benton, Vannice, & Vosshall, 2007; Couto, Alenius, & Dickson, 2005). *fipi* knockdown under the control of Or67d-GAL4 driver repeated the effects of Snmp-GAL4 driver demonstrating a decrease in the IPI value. At the same time, Or47b-GAL4 had no effects on IPI. An unexpected result was obtained with the Ir84a-GAL4 driver. *fipi* knockdown under the control of Ir84a-GAL4 led to an increase in IPI.

fipi *expression in the brain and olfactory neurons*

We immunostained brains and the third segments of antennas against FIPI using the polyclonal antibodies specified in the western blot experiments (Figure 7). Males with FIPI level decreased in the heads (knockdown Act5C-GAL4/UAS-RNAi and deletion stock fipi[362]) relative to the corresponding controls were analyzed. FIPI immunostaining in control and knockdown samples had a similar pattern. We did not find specific signal in both brains and antennas. We could just detected nonspecific signal from glial sheath of brain and nerves. To be more specific in the FIPI expression analysis we used *Drosophila* males with green fluorescent protein (GFP) fluorescence in distinct populations of olfactory neurons (Or67d-GAL4/UAS-GFP and Ir84a-GAL4/UAS-GFP). In antennae Or67d and Ir84a neurons (marked with GFP) did not demonstrate staining against FIPI. But there were a lot of immunoreactive material on the sensilla over the whole surface of the antennas in both control and experimental flies (fipi[361] vs. fipi[362], data not shown).

Discussion

In this study, all three experimental groups of flies with impaired expression of gene *CG15630* showed IPI reduction in the courtship song of *Drosophila* males (Figure 3). That is

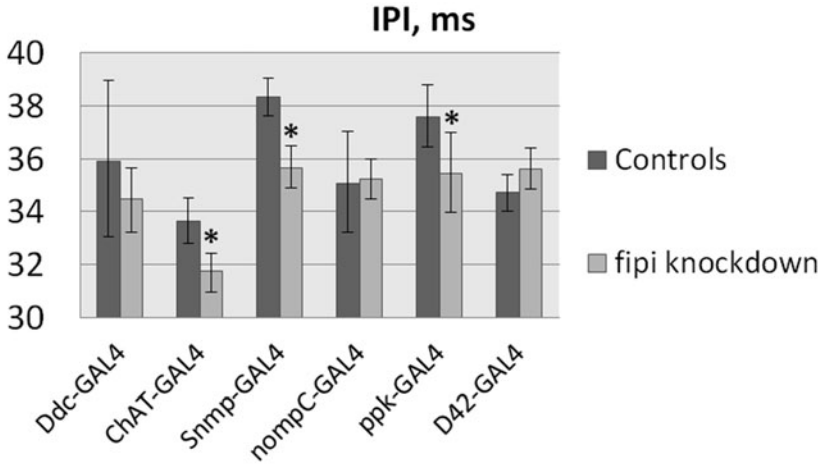

Ddc-GAL4	dopaminergic and serotonergic neurons
ChAT-GAL4	cholinergic neurons
Snmp-GAL4	olfactory sensory neurons of the antenna
nompC-GAL4	the class III dendritic arborization neurons, gentle-touch sensation
ppk-GAL4	peripheral sensory neurons
D42-GAL4	motor neurons

Figure 8. IPI in local fipi knockdowns (GAL4/UAS-RNAi) affecting various types of neurons. Mean values ($n = 20$) with 95% confidence intervals are shown. Significant differences from the corresponding GAL4/+ control are marked with asterisks (two-sided randomization test, $p < .05$). The cell specificity of GAL4 drivers is presented at the bottom.

why we named this gene the *factor of interpulse interval* (*fipi*). The *fipi[362]* deletion, on one hand, and *fipi* knockdown and *fipi[3404z]* P insertion, on the other, caused predictable consequences: formation of abnormal transcript resulted from splicing defect or essential reduction in the normal transcript level, respectively (Figure 5). It should be noted that the P insertion and *fipi[362]* deletion affect the first exon, and the hpRNA used for knockdown is complementary to the same first exon. At the same time *fipi* knockdown by means of RNAi against exon 6 (VDRC RNAi stock #37842) was lethal under Act5C-Gal4 driver and had no effect on IPI value under elav-Gal4 driver (BDSC stock #8765, unpublished data). The simplest explanation would be the existence of non-annotated *fipi* isoforms, but we did not find them in our northern and western blotting experiments. The antibodies against epitope in the second exon (unique amino acid sequence in *Drosophila* proteome) detected FIPI protein at significantly reduced level by western blotting in the *fipi* knockdown and *fipi[362]* deletion flies (Figure 7). Bioinformatic data indicate that the first exon of *fipi* possibly encodes the N- and H-regions of the signal peptide (14 of 19 amino acids, phobius.sbc.su.se) at the N-terminus of FIPI protein. So, *fipi[362]* deletion can potentially cause abnormal FIPI localization in neurons that alters their functioning. But we did not observe specific FIPI signal in the brains and antenna of fipi[362] flies (unpublished data). The significance of this amino acid sequence in FIPI remains to be established.

Courtship song assay revealed the most IPI decrease in flies with *fipi* knockdown under control of the Snmp-GAL4 driver (Figure 8). *Snmp* gene encodes a membrane protein, which is synthesized in the olfactory sensory neurons of trichoid sensilla in the antennae and the proboscis. *Snmp*-neurons include sensory cells involved in detection of 11-cis-vaccenyl acetate (cVa) through OR67d receptors (Benton *et al.*, 2007). *fipi* knockdown in OR67d neurons also resulted in IPI decrease reproducing the Snmp-GAL4 driver effect. cVa is a volatile pheromone of *Drosophila* males involved in regulation of social, particularly sexual, behavior. An increased sensitivity to this pheromone after unsuccessful experience of courting a mated female causes the suppression of courtship behavior (Keleman *et al.*, 2012). According to the high-throughput data of Graveley *et al.* (2011), sited at the electronic resource FlyBase (flybase.org), *Snmp* is expressed predominantly in the adult males and is not detected in the embryos and pupae. Thus, the effect of *fipi* knockdowns under Snmp-GAL4 and Or67d-GAL4 on male courtship song may be definitely linked to impaired reception of olfactory stimuli (including cVa) in the adult flies. This conclusion is consistent with our previous results showing IPI reduction in males with conditional *fipi* knockdown at the stage of imago (Fedotov *et al.*, 2014) and also with the fact of IPI reduction in flies with ChAT-GAL4 driven knockdown (Figure 8). Gene *ChAT* encodes choline acetyltransferase enzyme expressed in the cholinergic neurons (Kitamoto, Wang, & Salvaterra, 1998). Acetylcholine is the major excitatory neurotransmitter at all levels of the olfactory signal processing from sensory neurons to interneurons of the mushroom bodies (Gu & O'Dowd, 2006; Kazamam & Wilson, 2008; Yasuyama & Salvaterra, 1999).

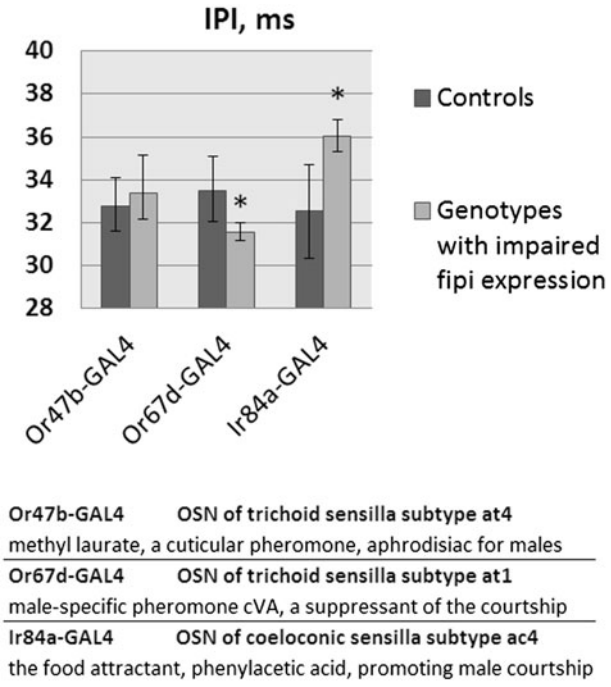

Figure 9. IPI in local *fipi* knockdowns (GAL4/UAS-RNAi) affecting three populations of OSN, expressing different olfactory receptor genes. Mean values ($n = 20$) with 95% confidence intervals are shown. Significant differences from the corresponding GAL4/+ control are marked with asterisks (two-sided randomization test, $p < .05$). The cell specificity of GAL4 drivers and chemosignals detected by the cells are presented at the bottom.

In the literature, we did not meet the data concerning possible impact of olfactory stimuli on IPI value of the courtship song. Recently, the neural network managing the initiation of courtship behavior was described (Clowney, Iguchi, Bussell, Scheer, & Ruta, 2015; Kohatsu, Koganezawa, & Yamamoto, 2011; von Philipsborn *et al.*, 2011). The courtship ritual is triggered by the integrative neurons P1 (15–20 cells) located in the posterior lateral neuropile. Activity of P1 neurons depends on several main inputs: the excitatory input from vAB3 from the gustatory receptors on the forelegs, the inhibitory input from mAL neurons and the inhibitory input from the olfactory sensory neurons. It was shown that the olfactory stimuli alone are not able to activate P1 neurons (Clowney *et al.*, 2015). On the contrary, the volatile pheromone cVa significantly suppresses the response of male P1 neurons to a virgin female. Thus, we suppose that a behavioral effect of *fipi* knockdown is caused by abnormalities in regulation of P1 neurons activity by the olfactory stimuli. Data from von Philipsborn *et al.* (2011, Table 1) implied that increase in activity of P1 neurons is accompanied by an increase in IPI. Reduced *fipi* expression may lead to a decrease in the activity of P1 neurons.

In the context of our suggestion about the FIPI function in the olfactory circuits, the revealed effects of *fipi* knockdown under ppk-GAL4 and Ir84a-GAL4 are interesting. In adult flies, ppk-GAL4 drives expression in sensory peripheral neurons of the body wall, legs, wings, antennae, proboscis, as well as in a number of sensory neurons associated with female reproductive tract and male gonads (Häsemeyer, Yapici, Heberlein, & Dickson, 2009; Rezával *et al.*, 2012; Yang *et al.*, 2009). In the reproductive tract of females, *ppk/fru* neurons detect sexual peptide that falls with the sperm of the male during copulation into the genital tract of the female that leads to the suppression of synaptic release and reduction of sexual receptivity (Häsemeyer *et al.*, 2009; Rezával *et al.*, 2012; Yang *et al.*, 2009). The effect of the *fipi* knockdown on courtship song pattern can also be associated with impaired reception of some chemical signals with *ppk* neurons in the male gonads or some chemosensory organs. At the same time *fipi* knockdown in population of the IR84a OSNs, detecting the food attractant phenylacetic acid and promoting male courtship (Grosjean *et al.*, 2011), resulted in an increase in IPI value, that is opposite to the effects of *fipi* knockdown under Or67d-GAL4 and ppk-GAL4 drivers. Thus, a proper *fipi* expression seems to be necessary for perception of sexual chemosignals, and the effect of *fipi* knockdown on IPI value depends on the type of chemoreceptor neurons affected. Grosjean *et al.* (2011) reported that IR84a olfactory receptor is expressed in FRU^{M}-positive neurons and $Ir84a^{GAL4}$ mutant males court wild type females significantly less than do wild-type males. The observed reduction in courtship index is highly comparable to the phenotype of flies in which all FRU^{M}-positive OSNs are silenced (Stockinger *et al.*, 2005), suggesting that IR84a-expressing neurons are the major olfactory fru^{M} channel contributing to this behavior. So the specific effects of *fipi* knockdown under Ir84-GAL4 may be related to its influence on FRU^{M} function in IR84a OSNs. The possibility of our suggestion is increased with evidence of increased IPIs between song pulses in *fru* mutant songs (Wheeler, Kulkarni, Gailey, & Hall, 1989).

The opposite effects of *fipi* knockdowns in different OSN population could be explained by specificity of *fipi* expression in the neurons. But we failed to detect FIPI in neuronal structures of Or67d and IR84a OSNs in the olfactory lobes of brain and antennas. FIPI antibodies perhaps could not penetrate glial sheath and/or bind non-FIPI protein on sheath. Besides, FIPI level could be exceedingly faint for fluorescent detection in the organ samples. We suppose FIPI detection in neurons by creating *fipi* promoter GAL4 flies will more promised approach in future studies.

NCAM2, the FIPI mammalian homolog, is known to play a role in the compartmental organization of axons and dendrites and target selection in the olfactory bulb (Alenius & Bohm, 2003; Borisovska, McGinley, Bensen, & Westbrook, 2011; Walz, Mombaerts, Greer, & Treloar, 2006). As FIPI, NCAM2 also has the small first exon coding for signal peptide and the large first intron, so further investigation of the *fipi* gene may be helpful for revealing the NCAM2 protein functions in neurons of mammals.

Acknowledgements

We thank the Bloomington Drosophila Stock Center (NIH P40OD018537) at Indiana University (USA) and the Vienna Drosophila RNAi Center at Campus Science Support Facilities (Austria) for providing us with transgenic GAL4 and RNAi fly stocks. We are grateful to Dr. Konstantin G. Iliadi (The Hospital for Sick Children, Toronto, ON, Canada) for propagation, maintenance, and transcontinental shipment of these stocks to our laboratory.

Disclosure statement

No potential conflict of interest was reported by the authors.

Funding

The study was funded by Russian Foundation for Basic Research according to the research Project No. 16-34-00028mol_a.

ORCID

Sergey A. Fedotov http://orcid.org/0000-0002-7428-120X
Julia V. Bragina http://orcid.org/0000-0003-0432-0063
Natalia G. Besedina http://orcid.org/0000-0003-0603-9486
Larisa V. Danilenkova http://orcid.org/0000-0001-7826-6106
Elena A. Kamysheva http://orcid.org/0000-0002-5301-2393
Nikolai G. Kamyshev http://orcid.org/0000-0002-3611-7417

References

Alenius, M., & Bohm, S. (2003). Differential function of RNCAM isoforms in precise target selection of olfactory sensory neurons. *Development*, *130*, 917–927. doi:10.1242/dev.00317

Andersson, L.S., Larhammar, M., Memic, F., Wootz, H., Schwochow, D., Rubin, C.-J., … Kullander, K. (2012). Mutations in *DMRT3* affect locomotion in horses and spinal circuit function in mice. *Nature*, *488*, 642–646. doi:10.1038/nature11399

Bennet-Clark, H.C. (1984). A particle velocity microphone for the song of small insects and other acoustic measurements. *Journal of Experimental Biology*, *108*, 459–463.

Benton, R., Vannice, K.S., & Vosshall, L.B. (2007). An essential role for a CD36-related receptor in pheromone detection in *Drosophila*. *Nature*, *450*, 289–293. doi:10.1038/nature06328

Bieschke, E.T., Wheeler, J.C., & Tower, J. (1998). Doxycycline-induced transgene expression during *Drosophila* development and aging. *Molecular Genetics & Genomics*, *258*, 571–579. doi:10.1007/s004380050770

Borgius, L., Nishimaru, H., Caldeira, V., Kunugise, Y., Low, P., Reig, R., … Kiehn, O. (2014). Spinal glutamatergic neurons defined by EphA4 signaling are essential components of normal locomotor circuits. *Journal of Neuroscience*, *34*, 3841–3853. doi:10.1523/JNEUROSCI.4992-13.2014

Borisovska, M., McGinley, M.J., Bensen, A., & Westbrook, G.L. (2011). Loss of olfactory cell adhesion molecule reduces the synchrony of mitral cell activity in olfactory glomeruli. *The Journal of Physiology*, *589*, 1927–1941. doi:10.1113/jphysiol.2011.206276

Burgess, A., Wainwright, S.R., Shihabuddin, L.S., Rutishauser, U., Seki, T., & Aubert, I. (2008). Polysialic acid regulates the clustering, migration, and neuronal differentiation of progenitor cells in the adult hippocampus. *Developmental Neurobiology*, *68*, 1580–1590. doi:10.1002/dneu.20681

Chintapalli, V.R., Wang, J., & Dow, J.A. (2007). Using FlyAtlas to identify better *Drosophila melanogaster* models of human disease. *Nature Genetics*, *39*, 715–720. doi:10.1038/ng2049

Clowney, E.J., Iguchi, S., Bussell, J.J., Scheer, E., & Ruta, V. (2015). Multimodal chemosensory circuits controlling male courtship in *Drosophila*. *Neuron*, *87*, 1036–1049. doi:10.1016/j.neuron.2015.07.025

Couto, A., Alenius, M., & Dickson, B.J. (2005). Molecular, anatomical, and functional organization of the *Drosophila* olfactory system. *Current Biology*, *15*, 1535–1547. doi:10.1016/j.cub.2005.07.034

Duff, M.O., Olson, S., Wei, X., Garrett, S.C., Osman, A., Bolisetty, M., … Graveley, B.R. (2015). Genome-wide identification of zero nucleotide recursive splicing in *Drosophila*. *Nature*, *521*, 376–379. doi:10.1038/nature14475

Dweck, H.K.M., Ebrahim, S.A.M., Thoma, M., Mohamed, A.A.M., Keesey, I.W., Trona, F., … Hansson, B.S. (2015). Pheromones mediating copulation and attraction in *Drosophila*. *Proceedings of the National Academy of Sciences of the United States*, *112*, E2829–E2835. Retrieved from www.pnas.org/cgi/doi/10.1073/pnas.1504527112

Edgington, E.S. (1995). *Randomization tests*. New York: Marcel Dekker.

Efron, B., & Tibshirani, R.J. (1993). *An introduction to the bootstrap*. London: Chapman & Hall.

Fedotov, S.A., Bragina, J.V., Besedina, N.G., Danilenkova, L.V., Kamysheva, E.A., Panova, A.A., & Kamyshev, N.G. (2014). The effect of neurospecific knockdown of candidate genes for locomotor behavior and sound production in *Drosophila melanogaster*. *Fly*, *8*, 176–187. doi:10.4161/19336934.2014.983389

Fore, T.R., Ojwang, A.A., Warner, M.L., Peng, X., Bohm, R.A., Welch, W.P., … Zhang, B. (2011). Mapping and application of enhancer-trap flippase expression in larval and adult *Drosophila* CNS. *Journal of Visualized Experiments*, *52*, e2649. doi:10.3791/2649

Goulding, M. (2009). Circuits controlling vertebrate locomotion: Moving in a new direction. *Nature Reviews Neuroscience*, *10*, 507–518. doi:10.1038/nrn2608

Graveley, B.R., Brooks, A.N., Carlson, J.W., Duff, M.O., Landolin, J.M., Yang, L., … Celniker, S.E. (2011). The developmental transcriptome of *Drosophila melanogaster*. *Nature*, *471*, 473–479. doi:10.1038/nature09715

Grosjean, Y., Rytz, R., Farine, J.-P., Abuin, L., Cortot, J., Jefferis, G.S.X.E., & Benton, R. (2011). An olfactory receptor for food-derived odours promotes male courtship in *Drosophila*. *Nature*, *478*, 236–240. doi:10.1038/nature10428

Gu, H., & O'dowd, D.K. (2006). Cholinergic synaptic transmission in adult *Drosophila* Kenyon cells *in situ*. *Journal of Neuroscience*, *26*, 265–272. doi:10.1523/JNEUROSCI.4109-05.2006

Häsemeyer, M., Yapici, N., Heberlein, U., & Dickson, B.J. (2009). Sensory neurons in the *Drosophila* genital tract regulate female reproductive behavior. *Neuron*, *61*, 511–518. doi:10.1016/j.neuron.2009.01.009

Huang, J., & Chen, F. (2006). Simultaneous amplification of 5′ and 3′ cDNA ends based on template-switching effect and inverse PCR. *BioTechniques*, *40*, 187–189. doi:10.2144/000112051

Iliadi, K.G., Kamyshev, N.G., Popov, A.V., Iliadi, N.N., Rashkovetskaya, E.L., Nevo, E., & Korol, A.B. (2009). Peculiarities of the courtship song in the *Drosophila melanogaster* populations adapted to gradient of microecological conditions. *Journal of Evolutionary Biochemistry and Physiology*, *45*, 579–588. doi:10.1134/S0022093009050041

Karim, M.R., Endo, K., Moore, A.W., & Taniguchi, H. (2014). Whole mount immunolabeling of olfactory receptor neurons in the *Drosophila* antenna. *Journal of Visualized Experiments*, *87*, e51245. doi:10.3791/51245

Kazamam, H., & Wilson, R.I. (2008). Homeostatic matching and nonlinear amplification at identified central synapses. *Neuron*, *58*, 401–413. doi:10.1016/j.neuron.2008.02.030

Keleman, K., Vrontou, E., Krüttner, S., Yu, J.Y., Kurtovic-Kozaric, A., & Dickson, B.J. (2012). Dopamine neurons modulate pheromone responses in *Drosophila* courtship learning. *Nature*, *489*, 145–149. doi:10.1038/nature11345

Kitamoto, T., Wang, W., & Salvaterra, P.M. (1998). Structure and organization of the *Drosophila* cholinergic locus. *Journal of Biological Chemistry*, *273*, 2706–2713. doi:10.1074/jbc.273.5.2706

Kohatsu, S., Koganezawa, M., & Yamamoto, D. (2011). Female contact activates male-specific interneurons that trigger stereotypic courtship behavior in *Drosophila*. *Neuron*, *69*, 498–508. doi:10.1016/j.neuron.2010.12.017

Kurtovic, A., Widmer, A., & Dickson, B.J. (2007). A single class of olfactory neurons mediates behavioural responses to a *Drosophila* sex pheromone. *Nature*, *446*, 542–546. doi:10.1038/nature05672

Landis, G.N., Bhole, D., Lu, L., & Tower, J. (2001). High-frequency generation of conditional mutations affecting *Drosophila melanogaster* development and life span. *Genetics*, *158*, 1167–1176.

Lu, T.Z., & Feng, Z.-P. (2012). NALCN: A regulator of pacemaker activity. *Molecular Neurobiology*, *45*, 415–423. doi:10.1007/s12035-012-8260-2

Nash, H.A., Scott, R.L., Lear, B.C., & Allada, R. (2002). An unusual cation channel mediates photic control of locomotion in *Drosophila*. *Current Biology*, *12*, 2152–2158. doi:10.1016/S0960-9822(02)01358-1

Pfaffl, M.W., Horgan, G.W., & Dempfle, L. (2002). Relative expression software tool (REST©) for group-wise comparison and statistical analysis of relative expression results in real-time PCR. *Nucleic Acid Research*, *30*, e36. doi:10.1093/nar/30.9.e36

Popov, A.V., Savvateeva-Popova, E.V., & Kamyshev, N.G. (2000). Peculiarities of acoustic communication in fruit flies *Drosophila melanogaster*. *Sensornye Systemy*, *14*, 60–74. [in Russian].

Rezával, C., Pavlou, H.J., Dornan, A.J., Chan, Y.B., Kravitz, E.A., & Goodwin, S.F. (2012). Neural circuitry underlying *Drosophila* female postmating behavioral responses. *Current Biology*, *22*, 1155–1165. doi:10.1016/j.cub.2012.04.062

Rutishauser, U. (2008). Polysialic acid in the plasticity of the developing and adult vertebrate nervous system. *Nature Reviews Neuroscience*, *9*, 26–35. doi:10.1038/nrn2285

Seidenfaden, R., Krauter, A., & Hildebrandt, H. (2006). The neural cell adhesion molecule NCAM regulates neuritogenesis by multiple mechanisms of interaction. *Neurochemistry International*, *49*, 1–11. doi:10.1016/j.neuint.2005.12.011

Stockinger, P., Kvitsiani, D., Rotkopf, S., Tirián, L., & Dickson, B.J. (2005). Neural circuitry that governs *Drosophila* male courtship behavior. *Cell*, *121*, 795–807. doi:10.1016/j.cell.2005.04.026

von Philipsborn, A.C., Liu, T., Yu, J.Y., Masser, C., Bidaye, S.S., & Dickson, B.J. (2011). Neuronal control of *Drosophila* courtship song. *Neuron*, *69*, 509–522. doi:10.1016/j.neuron.2011.01.011

Walmod, P.S., Kolkova, K., Berezin, V., & Bock, E. (2004). Zippers make signals: NCAM-mediated molecular interactions and signal transduction. *Neurochemical Research*, *29*, 2015–2035. doi:10.1007/s11064-004-6875-z

Walz, A., Mombaerts, P., Greer, C.A., & Treloar, H.B. (2006). Disrupted compartmental organization of axons and dendrites within olfactory glomeruli of mice deficient in the olfactory cell adhesion molecule, OCAM. *Molecular and Cellular Neuroscience*, *32*, 1–14. doi:10.1016/j.mcn.2006.01.013

Wheeler, D.A., Kulkarni, S.J., Gailey, D.A., & Hall, J.C. (1989). Spectral analysis of courtship songs in behavioral mutants of *Drosophila melanogaster*. *Behavior Genetics*, *19*, 503–528. doi:10.1007/BF01066251

Yang, C-h., Rumpf, S., Xiang, Y., Gordon, M.D., Song, W., Jan, L.Y., & Jan, Y.-N. (2009). Control of the postmating behavioral switch in *Drosophila* females by internal sensory neurons. *Neuron*, *61*, 519–526. doi:10.1016/j.neuron.2008.12.021

Yasuyama, K., & Salvaterra, P.M. (1999). Localization of choline acetyltransferase-expressing neurons in *Drosophila* nervous system. *Microscopy Research and Technique*, *45*, 65–79. doi:10.1002/(SICI)1097-0029(19990415)45:2<65::AID-JEMT2>3.0.CO;2-0